Strong angular dispersion using higher bands of planar silicon photonic crystals

Babak Momeni,[*] Maysamreza Chamanzar, Ehsan Shah Hosseini, Murtaza Askari, Mohammad Soltani, and Ali Adibi

School of Electrical and Computer Engineering, Georgia Institute of Technology, 777 Atlantic Dr NW, Atlanta, GA 30332, USA

[*]*Corresponding author: babak.momeni@osamember.org*

Abstract: We present experimental evidence for strong angular dispersion in a planar photonic crystal (PC) structure by properly engineering the modes in the second PC band. We show that by using the second photonic band of a square lattice PC, angular dispersion of 4°/nm can be achieved. We also show that major challenges in designing practical PC devices using second band modes can be addressed by engineering the lattice and adding input/output buffer stages designed to eliminate unwanted effects.

OCIS codes: (050.5298) Photonic Crystals; (130.3120) Integrated optics devices; (160.1245) Artificially engineered materials.

References and links

1. S. Fan, A. Mekis, S. G. Johnson, and J. D. Joannopoulos, "Manipulating light with photonic crystals," AIP Conf. Proc. **560**, 57–76 (2001).
2. T. F. Krauss, "Photonic crystals for integrated optics," AIP Conf. Proc. **560**, 89-98 (2001).
3. J. –J. He, B. Lamontagne, A. Delage, L. Erickson, M. Davies, and E. S. Koteles, "Monolithic integrated wavelength demultiplexer based on a waveguide Rowland circle grating in InGaAsP/InP," J. Lightwave Technol. **16**, 631-638 (1998).
4. S. Janz, A. Balakrishnan, S. Charbonneau, P. Cheben, M. Cloutier, A. Delâge, K. Dossou, L. Erickson, M. Gao, P. A. Krug, B. Lamontagne, M. Packirisamy, M. Pearson, and D.-X. Xu, "Planar waveguide Echelle gratings in silica-on-silicon," IEEE Photon. Technol. Lett. **16**, 503-505 (2004).
5. P. D. Trinh, S. Yegnanarayanan, F. Coppinger, and B. Jalali, "Silicon-on-insulator (SOI) phased-array wavelength multi/demultiplexer with extremely low-polarization sensitivity," IEEE Photon. Technol. Lett. **9**, 940-942 (1997).
6. T. Fukazawa, F. Ohno, and T. Baba, "Very compact arrayed-waveguide-grating demultiplexer using Si photonic wire waveguides," Jpn. J. Appl. Phys. 5B **43**, L673 - L675 (2004).
7. H. Kosaka, T. Kawashima, A. Tomita, M. Notomi, T. Tamamura, T. Sato, and S. Kawakami "Photonic crystals for micro lightwave circuits using wavelength-dependent angular beam steering," Appl. Phys. Lett. **74**, 1370-1372 (1999).
8. B. Momeni, J. Huang, M. Soltani, M. Askari, S. Mohammadi, A. Adibi, and M. Rakhshandehroo, "Compact wavelength demultiplexing using focusing negative index photonic crystal superprisms," Opt. Express **14**, 2413-2422 (2006).
9. H. Kosaka, T. Kawashima, A. Tomita, M. Notomi, T. Tamamura, T. Sato, and S. Kawakami, "Superprism phenomena in photonic crystals," Phys. Rev. B **58**, R10096-R10099 (1998).
10. H. Kosaka, T. Kawashima, A. Tomita, M. Notomi, T. Tamamura, T. Sato, and S. Kawakami, "Superprism phenomena in photonic crystals: Toward microscale lightwave circuits," J. Lightwave Technol. **17**, 2032-2038 (1999).
11. J. Witzens, T. Baehr-Jones, and A. Scherer, "Hybrid superprism with low insertion losses and suppressed cross-talk," Phys. Rev. E **71**, 026604-1-9 (2005).
12. T. Matsumoto, T. Asatsuma, and T. Baba, "Experimental demonstration of a wavelength demultiplexer based on negative-refractive photonic-crystal components," Appl. Phys. Lett. **91**, 091117 (2007).
13. S. G. Johnson, S. Fan, P. R. Villeneuve, J. D. Joannopoulos, and L. A. Kolodziejski, "Guided modes in photonic crystal slabs," Phys. Rev. B **60**, 5751-5758 (1999).
14. M. G. Moharam, E. B. Grann, D. A. Pommet, and T. K. Gaylord, "Formulation for stable and efficient implementation of the rigorous coupled-wave analysis of binary gratings," J. Opt. Soc. Amer. A **12**, 1068-1076 (1995).
15. B. Momeni and A. Adibi "Preconditioned superprism-based photonic crystal demultiplexers: analysis and design," Appl. Opt. **45**, 8466-8476 (2006).

#97089 - $15.00 USD Received 5 Jun 2008; revised 18 Aug 2008; accepted 21 Aug 2008; published 27 Aug 2008

16. Y. Vlasov and S. McNab, "Losses in single-mode silicon-on-insulator strip waveguides and bends," Opt. Express **12**, 1622-1631 (2004).

1. Introduction

Current demand for integration of multiple optical functionalities on a single chip has stimulated research activities on photonic crystals as *synthetic* optical materials in an integrated platform [1]. Multiple reports have recently been focused on using dispersive properties of photonic crystals to implement different device concepts. In particular, planar structures offer a viable platform for these devices, because of their compatibility with available integrated optical components as well as their manufacturability with the available well-developed microelectronics fabrication techniques [2]. In this work, our focus will be on the potentials of photonic crystal structures to realize ultra-compact and high-resolution integrated wavelength demultiplexers and on-chip spectrometers. Strong angular resolution is a key requirement for such applications, which translates into how efficient different wavelengths can be spatially separated inside the structure.

There have been different approaches for implementing optical wavelength demultiplexing and spectrometer devices, the most well-known of which are Echelle grating devices [3-4], array waveguide grating (AWG) structures [5-6], and those based on the superprism effect in photonic crystals [7]. Among these approaches, superprism effect offers the strongest dispersion and potentially, the most compact structures with very good spectral resolution for an on-chip spectrometer [8]. Since the introduction of the superprism effect [9,10], there have been several efforts in improving the performance of PC demultiplexers by using a multistage PC device [11,12] or by combining the superprism effects with PC dispersive properties (e.g., negative diffraction and negative refraction) [8]. Despite impressive recent progress, we believe that the full capacity of PC dispersive elements has not been yet utilized. One missing step in optimizing PC demultiplexers is the utilization of strong dispersive properties in higher photonic bands of planar PCs. The additional challenges that exist in using PCs in higher bands are the main reasons such devices have not been realized yet. Some of these challenges are: the difficulty of input/output coupling to the modes in higher PC bands, the possibility of multimode PC excitation at higher bands, and potentially higher insertion loss due to smaller mode group velocity.

In this paper, we discuss the feasibility of designing practical wavelength demultiplexers using the second band modes of planar PCs for achieving higher dispersion. We show that by proper engineering of the PC modes considerable improvement of the performance of these dispersive PC devices is achievable. We also address solutions to the major challenges for practical implementation of such PC devices.

2. Implementation

The PC structure that we will use throughout this paper is a square lattice PC of air holes in Si as shown by the scanning electron microscopy (SEM) image in Fig. 1(a). These structures are fabricated on a silicon on insulator (SOI) wafer with a silicon device layer of h = 220 nm thickness in which the optical signal is confined. This layer is sandwiched between two SiO_2 layers of 40 nm and 1 μm thickness on top and underneath, respectively. The oxide layer underneath optically isolates the device layer from the substrate silicon wafer. Figure 1(b) shows the calculated TE-like (with in-plane electric field) band structure (black solid curves) for the second band of a PC structure in such SOI wafers with PC hole radii of r = 96 nm and a lattice constant of a = 400 nm. Each curve (or iso-frequency contour) in the band structure shows the locus of possible in-plane wavevectors at a fixed wavelength shown on the curve. Two arrows on Fig. 1(b) show the directions of group velocity for two wavelengths corresponding to the PC modes excited inside the structure at a fixed incident angle of α = 25°. As expected, the direction of the group velocity is normal to the corresponding frequency contour at the point of excitation in the k_x-k_y plane. The very large superprism effect in this

#97089 - $15.00 USD Received 5 Jun 2008; revised 18 Aug 2008; accepted 21 Aug 2008; published 27 Aug 2008

structure is evident from the difference between the directions of these two arrows. The band structure in Fig. 1(c) is calculated using three-dimensional plane-wave expansion with 1470 plane wave components to assure its accuracy. The shaded region in Fig. 1(c) corresponds to the range of wavevectors that fall above the light line of the SiO_2 substrate layer, and thus, this region must be avoided. This no-confinement region is found by applying the

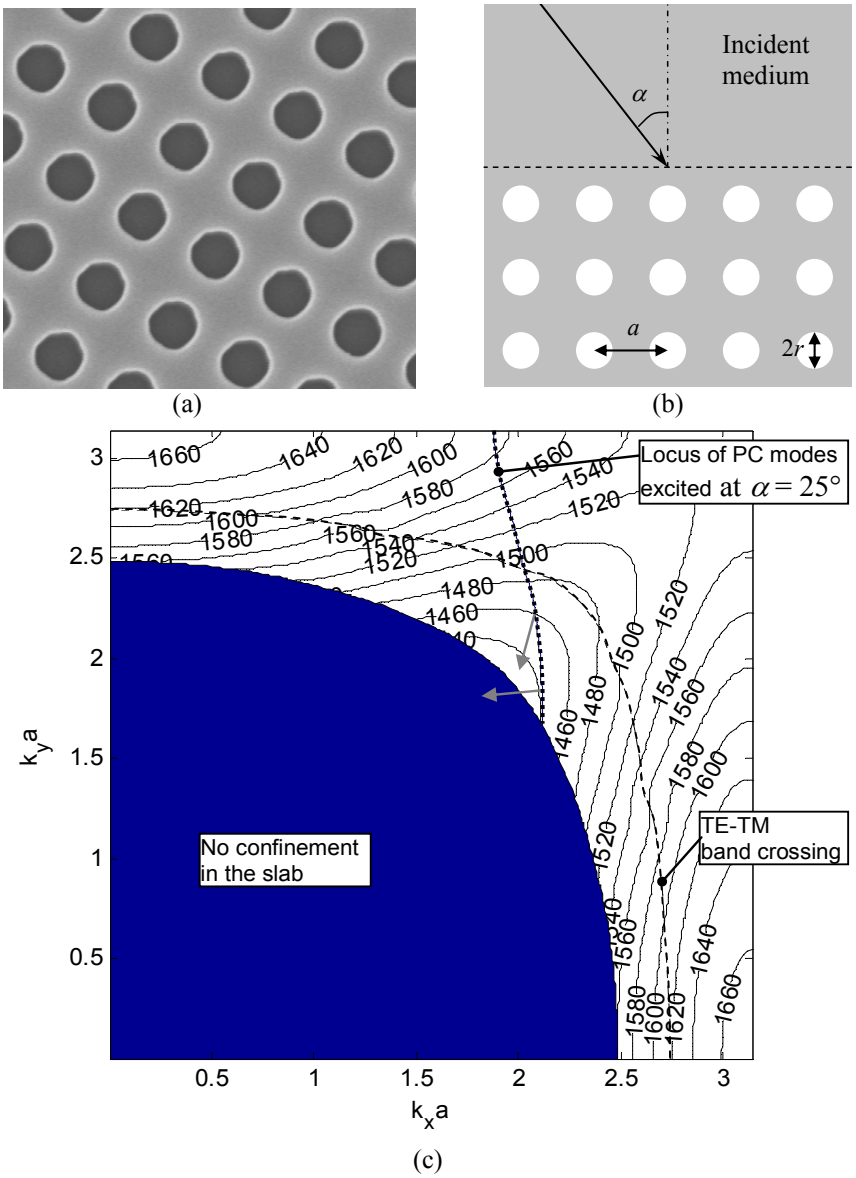

Fig. 1. (a) SEM image of a square lattice PC in a SOI wafer. (b) The excitation configuration is illustrated, in which the optical beam illuminates the PC interface at an incident angle of α. (c) Band structure of a square lattice PC structure in SOI with r = 96 nm and a = 400 nm is shown. The dotted line shows the locus of the modes excited in the PC with an incident wave from an unpatterned Si slab region on the same wafer at an incident angle of $\alpha = 25°$. The two arrows on this plot show the directions of the group velocities (normal to iso-frequency contours) inside the PC structure at wavelengths of 1460 and 1442 nm. Rapid change of the angle of group velocity with a small change in the incident wavelength is evident from this figure. The dashed line shows the cross section of TE-like and TM-like modes (the vicinity of this line must be avoided).

#97089 - $15.00 USD Received 5 Jun 2008; revised 18 Aug 2008; accepted 21 Aug 2008; published 27 Aug 2008

confinement criterion, $k_x^2 + k_y^2 > (2\pi n_{ox}/\lambda)^2$, in which n_{ox} is the refractive index of the isolating SiO_2 layer on the wafer, λ is the corresponding free-space wavelength of PC modes, and k_x and k_y are the in-plane wavevectors of PC modes in the x and y directions.

Assuming a plane wave at a specific incident angle [shown by α in Fig. 1(b)], we can use the electromagnetic boundary conditions at the PC boundary to find the k_x and k_y components of the wavevector of the mode excited inside the PC. The locus of these PC modes at different wavelengths is shown in Fig. 1(c) for the PC of interest at the incident angle of $\alpha = 25°$. Using this locus, we can calculate the direction of group velocity (i.e., the direction of propagation) inside the PC as a function of wavelength. Using Fig. 1(c), we can calculate the angular dispersion factor (i.e., the rate of change of the group velocity angle with wavelength) to be 6°/nm (This value is roughly estimated from the change in the angle of group velocity when wavelength is changed from 1440 nm to 1460 nm, and will be later confirmed in Fig. 4). This angular dispersion factor is considerably larger than the typical values observed in other devices (around 0.05-0.1°/nm in a grating spectrometer [3-4], 0.1-0.5°/nm in AWGs [5-6], and 0.7°/nm in the first photonic band of a PC-based device [8]).

Strong angular dispersion factor in the second photonic band of a planar PC, as shown in Fig. 1, suggests that this structure can be used, in principle, as a strongly dispersive optical material in a planar platform. However, for practical realization of such PC devices, some challenges need to be addressed. The first challenge is that to minimize propagation loss, the field must be confined to the Si slab region. To ensure this confinement, the operation range on the band structure in Fig. 1(c) will be limited to the portions of the band structure that are below the substrate (or cover) light cone [i.e., outside the shaded region in Fig. 1(c)]. This condition limits the operation range on the band structure and needs to be taken into account when designing such devices.

For practical implementations, we also need to make sure that the unpatterned Si slab and the PC structure remain single-mode in the frequency range of operation. This is particularly important when we work at higher photonic bands of the structure, where the ratio of the lattice constant (a) to the operation wavelength (λ) becomes larger. One way to achieve single-mode operation is to reduce the thickness of the Si slab. However, care must be taken in this process, as using thinner slabs results in lower confinement, and the available operation range on the band structure becomes even more limited. We have verified that for the parameters of the SOI structure analyzed in Fig. 1, the unpatterned Si slab is single-mode in the wavelength range of interest (i.e., wavelengths above 1400 nm). The simultaneous requirements for enough light confinement and single-mode operation, in practice, prevent us from going to higher frequency ranges and higher photonic bands. Therefore, we have limited our focus in this letter to the dispersion effects in the second TE-like photonic band of this planar PC structure. Furthermore, since the SOI structure used in our device is an asymmetric slab (due to the presence of SiO_2 substrate underneath the Si device layer), fields of the TE-like and TM-like modes of this structure are not orthogonal [13]. Therefore, mode gaps might open up when the TE-like photonic bands and TM-like photonic bands cross each other. Thus, to achieve proper operation of the dispersive component and to preserve the state of polarization, this cross-coupling region, marked by the dashed curve in Fig. 1(c), must be avoided (i.e., the locus of the operation points in the bandwidth of interest must not intersect the locus of TE-TM crossing).

Practical device realization also requires minimum light reflection at the interface of the PC structure and the incident region. There are two main mechanisms contributing to high reflection losses at PC interfaces. First, to operate at higher photonic bands, the wavelength of operation is relatively small (i.e., we are working at higher frequencies), and therefore, Floquet-type reflection orders will be excited in the incident region. These orders contribute to the loss by carrying some of the signal away from the target dispersive medium, and also, cause unwanted interference in the system by diffracting the light to unwanted directions in the incident region. The second cause of reflection loss is the impedance mismatch between the incoming wave and the modes of the highly dispersive PC in higher photonic bands. This

#97089 - $15.00 USD Received 5 Jun 2008; revised 18 Aug 2008; accepted 21 Aug 2008; published 27 Aug 2008

mismatch results in low transmission of the light to the target mode inside the PC region. To reduce reflection, we use a PC buffer stage to reduce these unwanted effects.

The schematic of our proposed PC buffer stage is shown in the inset of Fig. 2(a). In this buffer stage an intermediate PC region with half the period of our target dispersive PC is used at the input and output interfaces. In presence of these buffer PC layers, the tangential grating vector in the incident-buffer interface is large enough to make the first Floquet-type reflected order evanescent. Since the buffer stage works in the long wavelength regime, it effectively acts as an effective index medium with lower index compared to the input region. This lower effective index makes the first Floquet-type reflected order (i.e., $\mathbf{k}_{r,-1}$) at the buffer-PC interface also evanescent, and prevents such waves from propagating back to the input region. The main considerations in designing this buffer stage are having the hole sizes in the buffer stage large enough to make the first Floquet-type reflected order evanescent and keeping enough layers to avoid evanescent coupling of the (evanescent) reflected order to the input region. Figure 2(b) shows two-dimensional (2D) multilayer rigorous coupled wave simulation [14] results for transmission of TE-like wave (i.e., electric field inside the plane of periodicity) through the second photonic band of a square lattice PC device with r/a = 0.24 in Si. A refractive index of ε_r = 7.4 is used for Si in this simulation to account for the finite thickness (h = 220 nm) of the Si slab in the actual planar structure. The buffer stage has six layers of PC with r/a = 0.30 [as shown in the inset of Fig. 2(b)]; the angle of incident for the incident wave is α = 25°; and the input wave is incident from the top in the schematic view of Fig. 2(b). By comparing the transmission results for the cases with and without the buffer stage shown in Fig. 2(b), it can be seen that employing the buffer stage significantly improves the transmission. Note that in addition, by removing the unwanted reflected waves the inclusion of these devices as a part of a system involves less compatibility challenges.

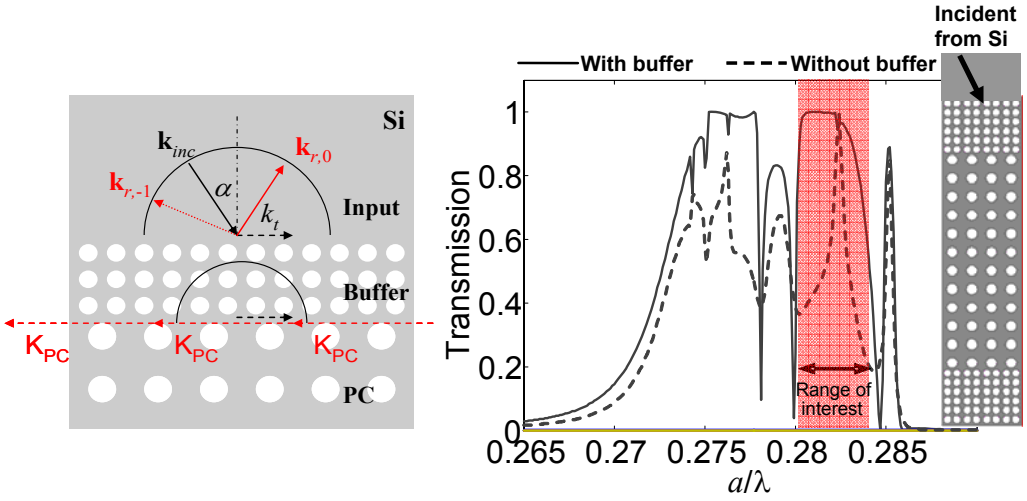

Fig. 2. (a) Wavevectors of the incident and refracted waves at the interface of a PC are schematically shown when a PC buffer stage is used. The half-circles in this figure show the dispersion diagram of each region at the operation frequency. The Floquet-type reflected order, $k_{r,-1}$, which is excited when no buffer stage is present is diminished, since it cannot propagate through the buffer stage. (b) Total transmission through the 2D photonic crystal structure shown in the inset is calculated with (solid curve) and without (dashed curve) the PC buffer stage. The operation is assumed in the second PC band, and the incident angle is α = 25°.

#97089 - $15.00 USD Received 5 Jun 2008; revised 18 Aug 2008; accepted 21 Aug 2008; published 27 Aug 2008

3. Experimental results

In order to test the possibility of forming practical PC demultiplexers using the second band PC modes, we used our findings in Figs. 1 and 2 to design a compact preconditioned PC demultiplexer [15] by engineering the PC to have the superprism effect, negative diffraction, and negative refraction simultaneously [8]. The design approach is the same as that explained in Ref. [15] and will not be repeated here. We have fabricated the designed square lattice PC structure using electron beam lithography and dry etching on an SOI wafer. The PC structure has a lattice constant a = 400 nm and holes with a normalized radius r/a = 0.24. The lattice constant in the PC buffer stage is a = 200 nm, and the holes in the buffer region have a normalized radius of r/a = 0.30. The SEM image of the fabricated structure is shown in Fig. 3. Figure 3(a) shows the close-up of the PC structure with buffer stage at the interfaces with Si, while Fig. 3(b) shows the output waveguide array fabricated to sample the output signal of the PC demultiplexer. These output waveguides are 3 μm apart and are tapered down from a 2.7 μm width at the sampling point to 1 μm at the edge of the sample; thus, there is negligible cross-coupling between them. In this demultiplexer, the input beam (with a beam waist of 6 μm) is broadened initially by propagation through an unpatterned Si slab region [on the left in Fig. 3(a)], such that after propagation through the PC structure (which is designed to have negative diffraction at the operation point) the beam is focused close to its diffraction-limited spot size at the output [8]. This output beam profile is sampled by an array of waveguides spaced 3 μm apart and carried to the output edge of the sample, as shown in Fig. 3(b).

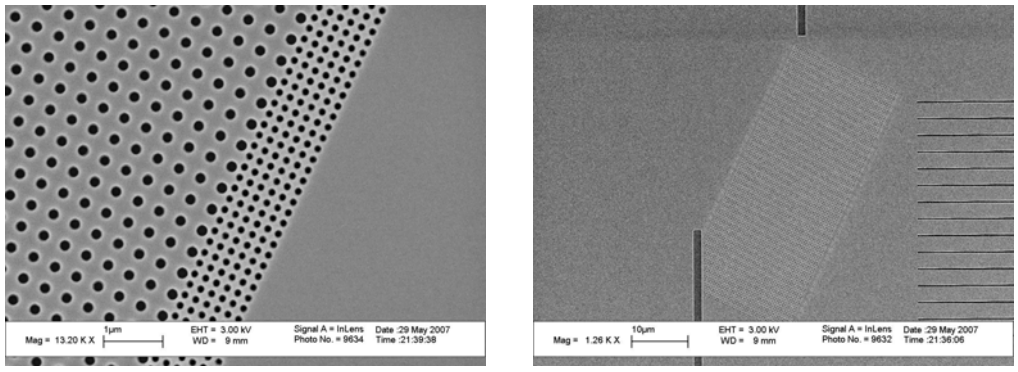

(a) (b)

Fig. 3. (a) SEM image of the interface of the PC demultiplexer is shown, revealing the details of the PC buffer stage. (b) Overall view of the photonic crystal device is shown. Six layers of small-period buffer PC are used at each interface to avoid unwanted Floquet-type transmission and reflection orders. The waveguides on the right (which are spaced 3 μm apart) sample the output optical beam profile and carry the signal to the output edge of the SOI device.

To measure the response of the system, light from a tunable laser is coupled to the structure through an input waveguide, and transmission through each of the output waveguides in the output array is measured using a standard lock-in technique as the input wavelength changes. The results of such measurements for four of the output waveguides are shown in Fig. 4(a). The wavelength at which the maximum transmission occurs for each of the output waveguides is the wavelength at which the beam is steered inside the PC structure towards that specific waveguide. The theoretical estimate of the refraction angles (i.e., the angle of group velocity inside the photonic crystal structure) and those measured in the experiment are plotted in Fig. 4(b). The observations from the experiment confirm the operation of the PC structure in the negative refraction regime and demonstrate strong angular dispersion factor (~4°/nm) close to what is predicted by theoretical estimates. Note that the experimental plot shows the location of the peak of the output beam profile as a function of

#97089 - $15.00 USD Received 5 Jun 2008; revised 18 Aug 2008; accepted 21 Aug 2008; published 27 Aug 2008

wavelength. Since this output beam profile is affected by higher-order diffraction effects, the location of the peak is different from the theoretical prediction of the angular dispersion (which relies only on the first-order effect). This fact causes the discrepancy between the theoretical and experimental plots in Fig. 4(b).

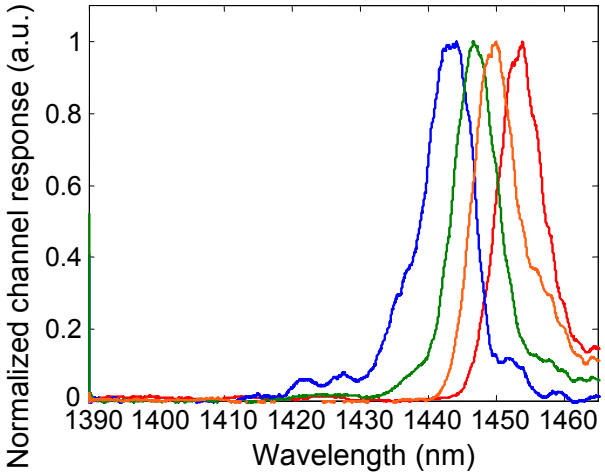

(a)

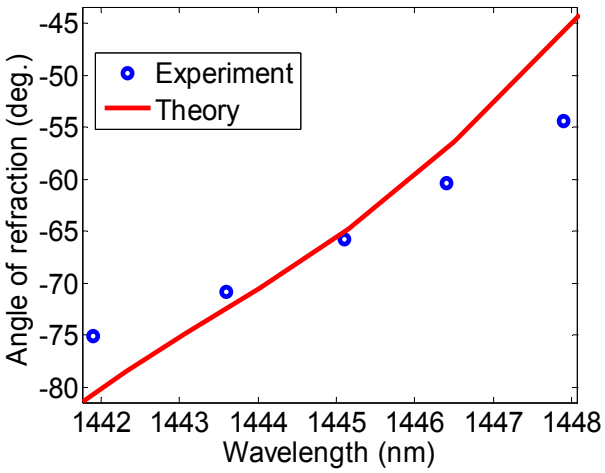

(b)

Fig. 4. (a) Channel responses for four of the output waveguides in the structure shown in Fig. 3 are measured and plotted after normalization. The wavelength of maximum transmission in each channel response presents the angle of refraction inside the PC corresponding to that wavelength. Plots of refraction angles inside the PC are plotted for different wavelengths using the experimentally measured transmission data (circles) and compared with those predicted from the band structure (solid curve).

Note that the main focus of this paper was the demonstration of the possibility of achieving very high angular dispersion using second band of the PCs, which was confirmed by the fabricated structure. A further systematic effort for the full optimization of the PC structures for the demultiplexer design by considering the trade-off among the resolution, propagation loss, and the device size is currently under investigation. Results in Fig. 4(a) show that the designed PC structure can separate channels with a 3-nm wavelength spacing

#97089 - $15.00 USD Received 5 Jun 2008; revised 18 Aug 2008; accepted 21 Aug 2008; published 27 Aug 2008

and a cross-talk of better than 2.4 dB. The PC structure used in this case was less than 20 μm x 50 μm in area. By increasing the size of the structure, better resolution and improved cross-talk level can be obtained. On the other hand, larger structures have higher propagation losses due to fabrication imperfections. Our estimated overall insertion loss in this fabricated device is 12-13 dB. This loss value is estimated by comparing the transmission through the superprism device with the transmission through a straight ridge waveguide on the same chip. However, with impressive recent advances in fabrication of PC structures [16] on one side, and optimization of designs to reduce other sources of loss, much better resolutions at reasonable insertion loss levels are foreseeable in near future. Nevertheless, these results are, to the best of our knowledge, the strongest angular dispersion experimentally demonstrated, and provide proof for the potentials of photonic crystals for realization of ultra-compact wavelength demultiplexers and spectrometers.

4. Conclusions

In this paper, we have addressed practical issues to be overcome for efficient demonstration of strong angular dispersion in a planar photonic crystal structure. We showed that by using dispersive properties of the second photonic band of a square lattice PC in an SOI wafer, strong angular dispersion (~4°/nm change in the refraction angle in a negative refraction regime) can be achieved. We also showed that the unwanted reflection and diffraction effects caused by operation at higher photonic bands can be avoided by designing a PC buffer stage. Using a simple design, we demonstrate a 20 μm × 50 μm PC demultiplexer with 3 nm resolution an at least 2.4 dB cross-talk isolation. These performance measures can be improved considerably by optimizing the PC demultiplexer. We believe that the results presented here can be used for designing compact PC demultiplexers and spectrometers with performances considerably better than current state of the art in all other PC based (and non-PC based) structures.

Acknowledgments

This work was supported by the Air Force Office of Scientific Research under Grant No. FA9550-07-1-0201 (G. Pomrenke) and by National Science Foundation under Contract No. ECCS-0742063.

#97089 - $15.00 USD Received 5 Jun 2008; revised 18 Aug 2008; accepted 21 Aug 2008; published 27 Aug 2008